ELSEVIER

Journal of Power Sources 96 (2001) 396–405

JOURNAL OF POWER SOURCES

www.elsevier.com/locate/jpowsour

Modeling lithium diffusion in nickel composite graphite

Venkat R. Subramanian, Ping Yu, Branko N. Popov, Ralph E. White*

Center for Electrochemical Engineering, Department of Chemical Engineering, University of South Carolina, Columbia, SC 29208, USA

Received 7 November 2000; accepted 11 November 2000

Abstract

A simple theoretical model is presented to simulate the galvanostatic discharge behavior of the Ni-composite graphite electrode. The discharge profiles predicted by using a constant diffusion coefficient (CDC) and by a varied diffusion coefficient (VDC) are compared in this paper. The results show that, the VDC model can be simplified to the CDC for discharge rates less than 2C for a 5 μm particle. Also, an approximate analytical solution is presented for VDC model, which is found to be valid for discharge rates up to 6C. Exchange current and diffusion coefficient for the lithium-diffusion are predicted.

Keywords: Ni-composite graphite electrode; Diffusion coefficient; Exchange current

1. Introduction

Li-ion batteries are now the preferred power sources for cellular phones, portable computers, and camcorders. The distinguished feature of lithium-ion batteries is the use of intercalation materials for both positive and negative electrodes. Because the intercalated species must transport from deep within the electrode to the surface to participate in electrochemical reactions that ultimately deliver energies, the particle size of the intercalation electrode plays an important role in determining the energy performance of the Li-ion cell [1]. For example, particles too large give rise to low energy densities at even moderate discharge rates [1,2]. In contrast, particles too small tend to be difficult to incorporate into electrode manufacturing processes. In the case of graphite negative electrode, particles too small also yield a high surface area, which eventually leads to a large irreversible capacity loss arising from the electrolyte decomposition [3,4]. Therefore, the particle size of the host material needs to be carefully designed to obtain the maximum battery energy. In designing lithium rechargeable batteries, some other parameters such as the electrode porosity, the lithium diffusion coefficient in the solid electrode, and the exchange current density of the electrode may also significantly influence the battery performance. Hence, a mathematical model taking into account these material properties is essentially required to give the insights of the physical processes occurring within the intercalation host and to predict theoretically the behavior of the intercalation host. This in turn can lead to a better development and design of the intercalation materials.

A number of models have been derived for analyzing the behaviors of insertion electrodes [5]. West et al. [6] derived a mathematical model that accounts for the coupled transport in the electrode and electrolyte phases during the charge and discharge of the TiS_2 porous electrode. Mao and White [7] extended West's model by including the mass transport across a separator. A complete model, in which the concentrated solution theory was incorporated, was derived by Doyle et al. [8] for simulating the discharge of a lithium electrode/polymer electrolyte/TiS_2 insertion cathode cell. Fuller et al. [9,10] and Doyle et al. [11] presented similar mathematical models for simulating the galvanostatic discharge of petroleum coke/electrolyte/$Li_yMn_2O_4$ dual lithium ion insertion cell, for studying the relaxation phenomena in petroleum coke/electrolyte/Li_yCoO_4 system, and for examining the behavior of the plastic lithium ion cells. A key approximation used in all these models is that the diffusion coefficient of insertion species is assumed to be constant over the entire concentration range, although the actual value of diffusion coefficient has been reported to be concentration-dependent [12–15]. Recently, Verbrugge and Koch [16,17] incorporated the variation of diffusion coefficient with concentration into a mathematical model to simulate the cyclic voltammograms and the galvanostatic intermittent titration process of the lithium intercalation in

* Corresponding author. Tel.: +1-803-777-4181; fax: +1-803-777-8265.
E-mail address: white@engr.sc.edu (R.E. White).

0378-7753/01/$ – see front matter
PII: S0378-7753(00)00657-1

Nomenclature

A_s	surface area of the electrode per unit volume (cm^2/cm^3)
C_s^0	initial (reference) lithium concentration in carbon insertion host (mol/cm^3)
D_e	diameter of the electrode (cm)
D_I^0	chemical diffusion coefficient of lithium in solid graphite at the infinite dilute state (cm^2/s). Found out to be ($\geq 1.25 \times 10^{-9}$ cm^2/s)
F	Faraday's constant (96487 C/equivalent)
$f(X_I)$	function of diffusion coefficient dependence on the concentration
i_p	local current density on the particle surface (A/cm^2)
$i_{o,ref}$	local reference exchange current density (A/cm^2)
I	macro current density of the electrode (A/g)
$I_{o,ref}$	macro reference exchange current density (A/g)
j	integer number in Eq. (13)
k	integer number in Eq. (4)
L	thickness of the electrode (cm)
m_e	mass of the electrode (g)
M_w	molecular weight of graphite (12 g/mol)
N	integer number in Eq. (4), (here $N = 8$)
Q	amount of charge passed to the graphite electrode, $Q = It$ (Ah/g)
r	radial coordinate of a spherical particle (m)
R	universal gas constant (8.3143 J/mol/K)
R_p	particle radius (cm)
t	time (s)
U	electrode potential relative to Li^+/Li (V)
V_e	geometric volume of the electrode (cm^3)
x	stoichiometric number in Li_xC_6
X_I	fractional occupancy of lithium in graphite host ($0 \leq X_I < 1$)
X_I^0	initial fractional occupancy of lithium ion in graphite, obtained by the ratio of the full discharge capacity to the theoretical capacity of graphite (372 mA h/g)
$X_{I,S}$	fractional occupancy of lithium ion on the particle surface
y	dimensionless radial coordinate

Greek letters

β	symmetric factor (= 0.5)
ε	porosity of the electrode
γ_I	activity coefficient
λ_j	root of $\tan \lambda = \lambda$, $j = 1, 2, \ldots, \infty$
ρ	specific density of graphite (g/cm^3)
τ	dimensionless time
Γ_k	polynomial fitting parameter, $k = 1, 2, \ldots, 8$
Ω_k	self-interaction coefficient, $k = 2, 3, \ldots, N$ (in this work $N = 8$)
Φ	open-circuit potential relative to Li^+/Li (V)
Φ^0	concentration-independent potential of the graphite electrode relative to Li^+/Li (V)
Φ_s	thermodynamic potential, defined in Eq. (4) (V)
Ψ	dimensionless parameter denoting the ratio of diffusional resistance of lithium ions in the particle to the interfacial kinetic resistance, defined in Eq. (15)

the carbon fiber, however, how the varied diffusion coefficient affects the predicted result was not illustrated in their model.

In this work, a simple mathematical model for the galvanostatic discharge process of lithium in graphite porous electrode is developed. The model developed is further used to analyze the effects of design parameters on the lithium intercalation into graphite.

2. Experimental

The model simulation was performed on the system of a porous graphite pellet electrode, which was used as a lithium intercalation host. The porous electrode was made of Ni-composite graphite powder, which was synthesized by electroless deposition of 10 wt.% thin nickel-composite coating (approximate 1 nm in thickness) [18] on the surface of graphite KS10 (10 μm, Timcal America). The Ni-composite coating on graphite was utilized to reduce the irreversible capacity loss of graphite in the initial cycle. Since the coating does not impede the lithium intercalation into graphite, the presence of Ni-composite coating does not affect the predicted charge performance of the graphite.

The graphite pellet electrode was prepared by mixing the Ni-composite graphite powder with 6 wt.% poly(vinylidene fluoride) (PVDF, Aldrich) powder and 1-methyl-2-pyrrolidinone solvent on a stainless steel current collector and dried under vacuum at 150°C for 12 h. The obtained pellet is about 9.9 mg in weight, 1.26 cm in diameter and 94 μm in thickness. The volume of this pellet electrode is calculated to be 0.0117 cm^3. The electrolyte consists of 1 M $LiPF_6$ in a 1:1:3 mixture of PD/EC/DMC with less than 15 ppm H_2O and 80 ppm HF (EM Inc.).

The galvanostatic charge–discharge experiment was conducted in a Swagelok three-electrode cell, in which the graphite pellet served as a working electrode and lithium metal foil was used as a reference electrode as well as a counter electrode. The experiments were carried out at 25°C using the EG&G PAR Potentiostat/galvanostat Model 273A driven by the CorrWare software system from Scribner Associates, Inc. The galvanostatic charge–discharge data were collected after cycling three times to ensure that stable and reproducible behavior had been obtained.

3. Diffusion model

The Ni-composite graphite particles in the porous graphite pellet electrode are assumed to be in spherical shape. The electrochemical reaction occurring at the individual particle surface is described as

$$x\mathrm{Li}^+ + x\mathrm{e}^- + \mathrm{C}_6 \underset{\text{Discharge}}{\overset{\text{Charge}}{\rightleftarrows}} \mathrm{Li}_x\mathrm{C}_6 \tag{1}$$

where x is a stoichiometric number of lithium intercalated into the graphite host. Upon charging the graphite, lithium ions diffuse from the electrode surface into the graphite insertion site. The reverse process occurs during the discharging process. To simplify the analysis, only the electrochemical intercalation/deintercalation reactions shown in reaction 1 are considered in this model. The side reactions such as the electrolyte decomposition and lithium metal deposition are neglected. The diffusion of lithium ions inside the spherical particle, can be represented by Fick's second law:

$$\frac{\partial X_\mathrm{I}}{\partial t} = \frac{D_\mathrm{I}^0}{r^2}\frac{\partial}{\partial r}\left(f(X_\mathrm{I})r^2\frac{\partial X_\mathrm{I}}{\partial r}\right) \tag{2}$$

where X_I denotes the fractional occupancy of lithium ions in total available sites of the insertion host, $X_\mathrm{I} = Q/372$, where Q and 372 mA h/g are the actual capacity and the theoretical capacity of lithium in graphite, respectively. The value of X_I ranges from 0 to 1. $X_\mathrm{I} = 1$ refers to the state that lithium occupies all the available sites, which corresponds to the capacity of 372 mA h/g and r is the radial distance from the center of the particle and $f(X_\mathrm{I})$ is the concentration dependence of the diffusion coefficient.

The open circuit potential (Φ) of the lithiated graphite electrode relative to the metallic lithium can be formulated as a function of the lithium fractional occupancy at the particle surface [16,17]:

$$\Phi = \Phi^0 + \frac{RT}{F}\ln\frac{1-X_{\mathrm{I,S}}}{X_{\mathrm{I,S}}} - \sum_{k=2}^{N}\frac{\Omega_k}{F}kX_{\mathrm{I,S}}^{k-1} \tag{3}$$

where Φ^0 refers to the electrode potential at the infinite dilute state of lithium in graphite [16], i.e. at $X_{\mathrm{I,S}} \to 0$ and R, T are the universal gas constant and temperature, respectively.

The thermodynamics of lithium intercalations into a solid insertion host departs from the Nernst equilibrium because the concentrations of the intercalated species are higher than the dilute value assumed at the standard state [10,16]. The parameter Ω_k in Eq. (4) is determined by fitting Eq. (3) to the experimental curve of the open-circuit potential of graphite versus the lithium occupancy using a least square polynomial regression method. Rewriting Eq. (3)

$$\Phi = \Phi_\mathrm{s} + \frac{RT}{F}\ln\frac{1-X_{\mathrm{I,S}}}{X_{\mathrm{I,S}}}, \quad \text{where} \quad \Phi_\mathrm{s} = \Phi^0 - \sum_{k=2}^{N}\frac{\Omega_k}{F}kX_{\mathrm{I,S}}^{k-1} \tag{4}$$

Since, there is a difficulty in collecting the actual equilibrium data of the carbon electrode in a finite period of time, the charging potential profile at a low charge current has been assumed to be an equilibrium potential profile and used to determine the thermodynamic parameters for the modeling simulation [8–11]. The open-circuit potential profile is obtained by charging the graphite system at C/40 rate (9.3 mA/g), which is lower than the rate of C/24 (i.e. 15.5 mA/g) known to be sufficiently slow to attain the near-equilibrium condition on graphite [1]. Fig. 1 presents

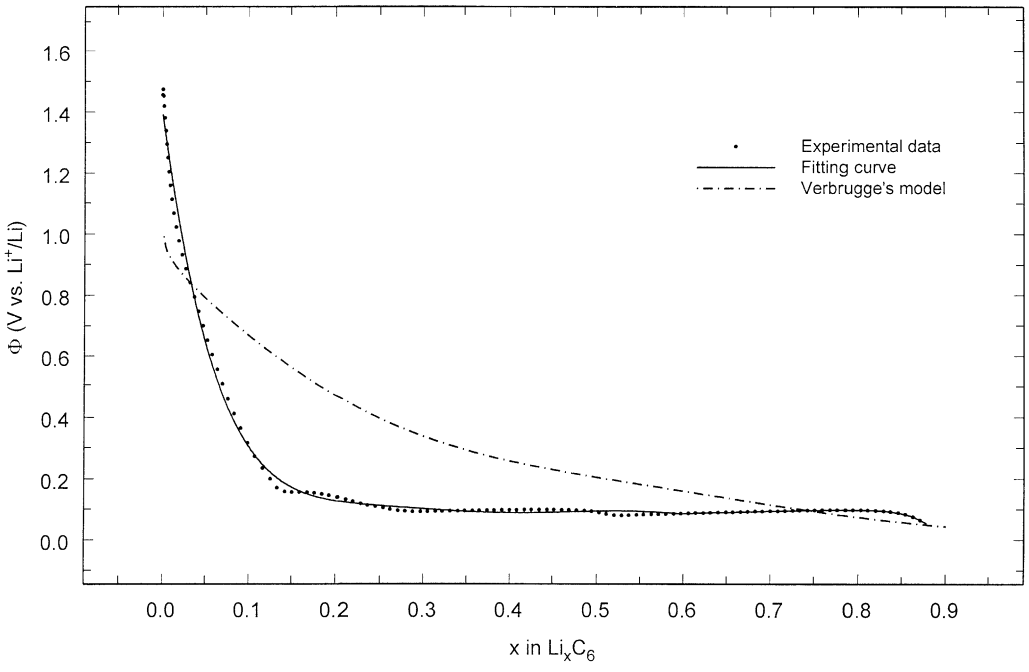

Fig. 1. Open-circuit potential as a function of the composition (x) in $\mathrm{Li}_x\mathrm{C}_6$.

Table 1
Activity coefficients

Material	Our result Graphite powder	Verbrugge's result Partially graphitic carbon fiber
Φ^0 (V)	1.3935	0.817
Φ_2/F (V)	10.6885	0.9926
Φ_3/F (V)	50.8584	0.8981
Φ_4/F (V)	148.8472	−5.630
Φ_5/F (V)	270.356	8.595
Φ_6/F (V)	296.0333	−5.784
Φ_7/F (V)	−178.537	1.468
Φ_8/F (V)	45.4660	

the experimentally thermodynamic data of graphite. The thermodynamic data for partially graphitic carbon fiber by Verbrugge [16] is also plotted for comparison. Note that, a plateau at the potential of 0.1 V versus Li^+/Li which characterizes the stage phenomena of lithium graphite intercalation compound (Li-GIC), is observed in the solid dot curve for graphite, while no significant plateau displays for partially graphitic carbon fiber. The solid dot data of graphite are fitted to Eq. (4) using a polynomial regression method and the resulted fitting curve is depicted as a solid line in Fig. 1. The values of potential Φ^0 and the interaction coefficients Ω_k/F ($k = 2$–8) are determined and summarized in Table 1. The values obtained by Verbrugge [16] are also included in Table 1 for comparison. The differences in the potential and interaction coefficients probably arise from the different materials used for lithium intercalation. As seen in Fig. 1, the lithium intercalation in graphite powder electrode mainly occurs at 0.1 V versus Li^+/Li while the lithium intercalation in partially graphitic carbon occurs from 0.8 V versus Li^+/Li and continues over the potential range of 0.1–0.8 V versus Li^+/Li. These different intercalation potentials could result in the different values of Φ^0 and Ω_k/F for the partially graphitic carbon and the graphite powder as shown in Table 1.

The function of diffusion coefficient dependence on the concentration is obtained [17] as

$$f(X_I) = \frac{D_I(X_I)}{D_I^0} = 1 + \frac{d\ln\gamma_I}{d\ln X_I} = -X_I(1-X_I)\frac{F}{RT}\frac{\partial\Phi}{\partial X_I} \quad (5)$$

where γ_I is the activity coefficient of lithium in the solid graphite host. The thermodynamic data of Ni-composite graphite in Fig. 1 were differentiated with X_I using a five-point finite difference method (accurate to the order h^4) to obtain the values of $\partial\Phi/\partial X_I$ at different concentration. The values of $f(X_I)$ at various X_I were calculated from Eq. (5) and plotted as a solid line in Fig. 2. Note that, three peaks in Fig. 3 are observed at the concentration X_I of about 0.09, 0.22, and 0.51. These X_I values as shown in Fig. 1 are in the ranges that the potential quickly drops, which corresponds to the stage transform of lithium intercalates. This result indicates that the significant variation of the lithium diffusion coefficient in graphite occurs at the state of the stage transform. The solid line of Fig. 2 is separated into five pieces and is regressed using a polynomial regression method to obtain the expression of $f(X_I)$

$$f(X_I) = \sum_{k=1}^{8} \Gamma_k X_I^k \quad (6)$$

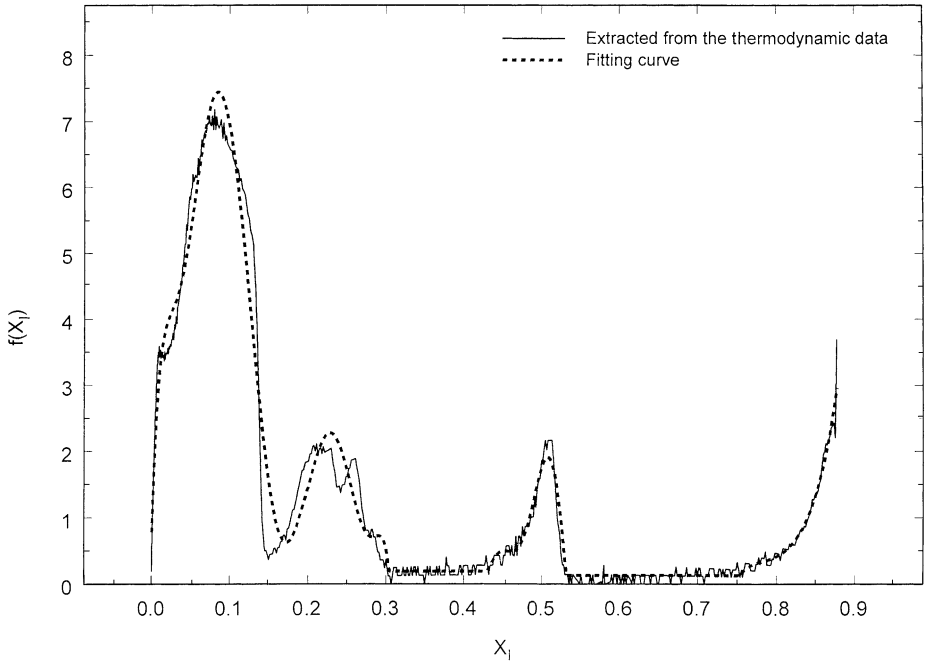

Fig. 2. Diffusion coefficient as a function of fractional occupancy.

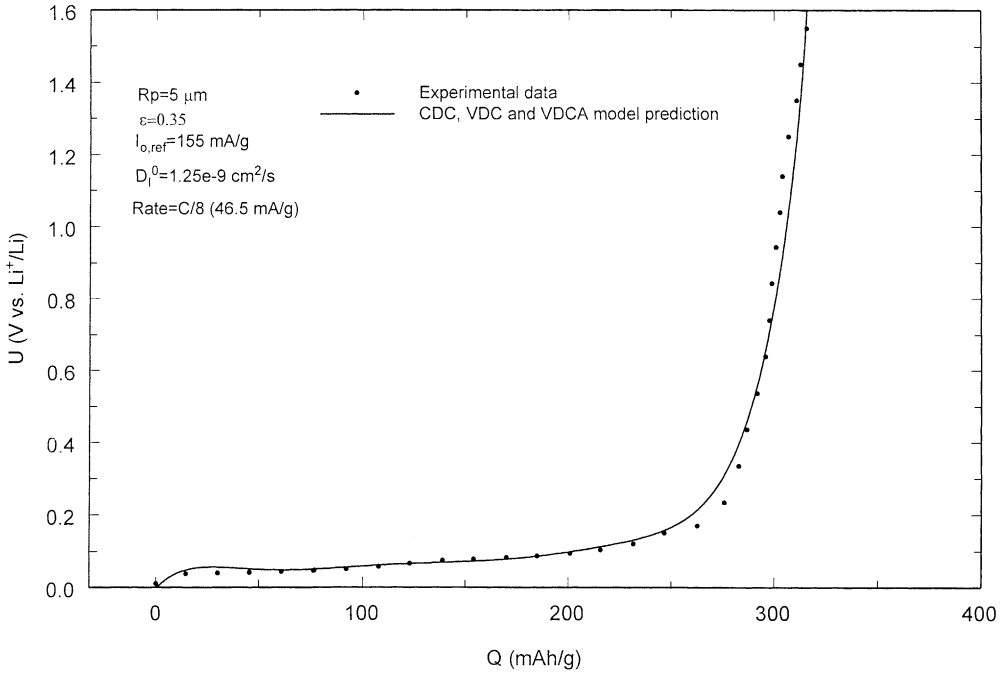

Fig. 3. Comparison of the experimental and the simulated discharge profile at the discharge rate of C/8 (i.e. 46.5 mA/g).

The fitted curve is depicted as the dotted line in Fig. 3. The corresponding fitting parameters of Γ_k are summarized in Table 2.

The discharge process starts from the fully charged state in which all the lithium ions uniformly distribute in the graphite particle with a fractional occupancy of X_I^0. The value of X_I^0 is obtained by the ratio of the full charge capacity to the theoretical capacity.

$$\text{at } t = 0, \quad X_I = X_I^0 \tag{7}$$

and the boundary conditions are

$$\text{at } r = 0, \frac{\partial X_I}{\partial r} = 0 \tag{8}$$

$$\text{at } r = R_p, \quad D_I^0 C_s^0 \frac{\partial X_I}{\partial r} = -\frac{i_p}{Ff(X_I)} \tag{9}$$

where F is the Faraday's constant. C_s^0 is the initial (reference) lithium concentration in graphite host, calculated with the fractional occupancy of lithium at fully insertion state (X_I^0), the specific density (ρ) and the molecular weight (M_w) of graphite from the expression [19]

$$C_s^0 = \frac{X_I^0 \rho}{6 M_w} \tag{10}$$

where, 6 refers to the stoichimetric number of carbon in Li_xC_6.

In Eq. (9), i_p denotes the local current density on the particle surface in terms of A/cm^2. The value of i_p is calculated with respect to the macro current density of the electrode, I (A/g), the mass of the electrode, m_e (g), the surface area of the electrode per unit volume, A_s (cm^2/cm^3), the geometric volume of the electrode, V_e (cm^3), and the electrode porosity ε, [20] as

$$i_p = \frac{I m_e}{A_s V_e (1 - \varepsilon)} \tag{11}$$

Table 2
Fitted values of Γ_k

	$0 < X_I \leq 0.303$	$0.303 < X_I \leq 0.430$	$0.431 < X_I \leq 0.530$	$0.530 < X_I \leq 0.755$	$0.775 < X_I \leq 0.877$
Γ_0	0.773639563	0.19	247332.207972	0.13	−17977.4156
Γ_1	408.1776515	0	−1660960.478778	0	78323.91484
Γ_2	−20856.54417	0	212827.412501	0	−109505.6582
Γ_3	544047.5498	0	21964243.996622	0	51468.93968
Γ_4	−7112522.79	0	−43752723.673841	0	−55839.23733
Γ_5	49518548.04	0	−75525635.243337	0	130202.4323
Γ_6	−187970332.8	0	367915176.568545	0	−58880.87905
Γ_7	368041823.4	0	−472426675.845534	0	−55749.27299
Γ_8	−291326139.5	0	210250890.426413	0	38051.47385

The surface area of the electrode per unit volume (A_s) is related to the radius of the spherical particle, R_p, and the electrode porosity

$$A_s = \frac{3(1-\varepsilon)}{R_p} \tag{12}$$

Three types of models are described here.

3.1. Constant diffusion coefficient (CDC)

The diffusion Eq. (2), with the initial and boundary conditions given by Eqs. (7)–(9), for constant diffusion coefficient (CDC) can be conveniently solved by means of variables separation [20–22] as

$$X_I = X_I^0 - \frac{i_p R_p}{F D_I^0 C_s}\left[3\frac{tD_I^0}{R_p^2} + \frac{1}{10}\left[5\left(\frac{r}{R_p}\right)^2 - 3\right] - 2\frac{R_p}{r}\sum_{j=1}^{\infty}\frac{\sin(\lambda_j r/R_p)}{\lambda_j^2 \sin(\lambda_j)}\, e^{-\lambda_j^2 (tD_I^0/R_p^2)}\right] \tag{13}$$

where the λ_j is the root of $\tan\lambda = \lambda\,(j = 1, 2, \ldots, \infty)$ [20–22]. Eq. (13) can be written in the dimensionless form

$$X_I = X_I^0 - \Psi\left[3\tau + \frac{1}{10}(5y^2 - 3) - \frac{2}{y}\sum_{j=1}^{\infty}\frac{\sin(\lambda_j y)}{\lambda_j^2 \sin(\lambda_j)}\, e^{-\lambda_j^2 \tau}\right] \tag{14}$$

with the dimensionless variables

$$\Psi = \frac{i_p R_p}{F D_I^0 C_s}, \qquad y = \frac{r}{R_p}, \qquad \tau = \frac{tD_I^0}{R_p^2} \tag{15}$$

Ψ denotes the ratio of the diffusional resistance of lithium ions in the particle to the interfacial kinetic resistance. When $\Psi \ll 1$, the diffusion resistance within the graphite particle is less important. On the other hand, when $\Psi > 1$, it is possible for the charge–discharge of the electrode to be limited by the diffusion of lithium within the graphite insertion electrode. This limitation often occurs at the high rate of early cells using nonporous thin film [23]. The lithium fractional occupancy at the particle surface, $X_{I,S}$, is obtained by substituting $y = 1$ into Eq. (14)

$$X_{I,S} = X_I^0 - \Psi\left[3\tau + 0.2 - 2\sum_{j=1}^{\infty}\frac{1}{\lambda_j^2}\, e^{-\lambda_j^2 \tau}\right] \tag{16}$$

3.2. Variable diffusion coefficient (VDC)

When the diffusion coefficient varies at different concentration as $D_I = D_I^0 f(X_I)$, the diffusion Eq. (2) with the initial/boundary conditions (Eqs. (7)–(9)) is solved numerically using finite differences in y and integrating the resulting nonlinear Ordinary differential equations (ODEs) using Maple [24]. The Maple program uses 40 node points in y-axis. The time taken for this program in an 833 MHz, 512 MB RAM, dual Pentium processor is less than 1 min. The same program can be used to obtain the discharge profiles for CDC models also.

3.3. Variable diffusion coefficient-approximate solution (VDCA)

An approximate solution for this concentration dependent diffusion case, [25,26] can be obtained by assuming that the concentration inside the particle is parabolic in nature. The details regarding the derivation can be found in [25,26].

$$\tau = \frac{1}{15}\frac{5f(X_{I,S})(1 - X_{I,S}) - \Psi}{f(X_{I,S})} \tag{17}$$

The accuracy of this expression depends on both Ψ and $f(X_I)$. Note that $X_{I,S}$ is given by a non-linear implicit algebraic expression in Eq. (17). For higher values of Ψ, one can use higher order approximations [25,26].

3.3.1. Electrokinetics

The kinetic of charge-transfer reaction occurring on the particle surface is described by the Butler–Volmer equation, which relates the local current density (i_p) to the surface overpotential (η_s) [17] as

$$i_p = i_{o,ref}(1 - X_{I,S})^{(1-\beta)}(X_{I,S})^{\beta}\left\{\exp\left[\frac{(1-\beta)F}{RT}\eta_s\right] - \exp\left[-\frac{\beta F}{RT}\eta_s\right]\right\} \tag{18}$$

where β is the symmetric factor ($\beta = 0.5$ here) and $i_{o,ref}$ is the local reference exchange current density in terms of A/cm^2. The overpotential (η_s) is specified from Eq. (4)

$$\eta_s = U - \Phi = U - \left[\Phi_s + \frac{RT}{F}\ln\frac{1 - X_{I,S}}{X_{I,S}}\right] \tag{19}$$

Eqs. (16) and (19) are the governing equations for the dependent variables $X_{I,S}$ and U at the different time, when a constant diffusion coefficient (CDC) is assumed. Upon discharging at a time t, the lithium fractional occupancy at the surface of particle, $X_{I,S}$, is determined first. Then, from Eq. (19) the electrode potential, U is obtained. The potential U is plotted as a function of the discharge capacity given by $Q = It$.

In the case of a varied diffusion coefficient (VDC), the surface concentration distribution with time is obtained numerically and the potential, U is obtained later from Eq. (19). Alternatively Eq. (17) is used for finding the surface concentration in the VDCA model.

4. Results and discussion

The basic parameter data used for the modeling simulation are listed in Table 3. The parameters measured

experimentally are based on Ni-composite coated KS10 graphite and the manufactured data are obtained only for bare KS10 graphite. The simulation process starts from the fully charged state in which the capacity of lithium ions in the graphite host is obtained to be 326 mA h/g at a charging rate of C/40, i.e. 9.3 mA/g (C rate refers to 372 mA/g of a current density). The initial (reference) lithium fractional occupancy (X_I^0) is determined to be 0.877 by taking the ratio of this capacity over the theoretical capacity of graphite (372 mA h/g). The lithium reference concentration, C_s^0 is determined to be 0.027 by applying the values of 0.877 for X_I^0, 2.21 g/cm^3 for ρ, and 12 g/mol for M_w into Eq. (10). The initial guesses for the diffusion coefficient, D_I^0, and the reference exchange current density, $I_{o,ref}$, are arbitrary. These two values are, then predicted accurately using the model simulation.

The predicted discharge potential profile and the experimental curve as a function of discharge capacity are plotted in Fig. 3 for C/8 rate. The dotted line is experimental data and the solid line is the simulated result. All of CDC, VDC

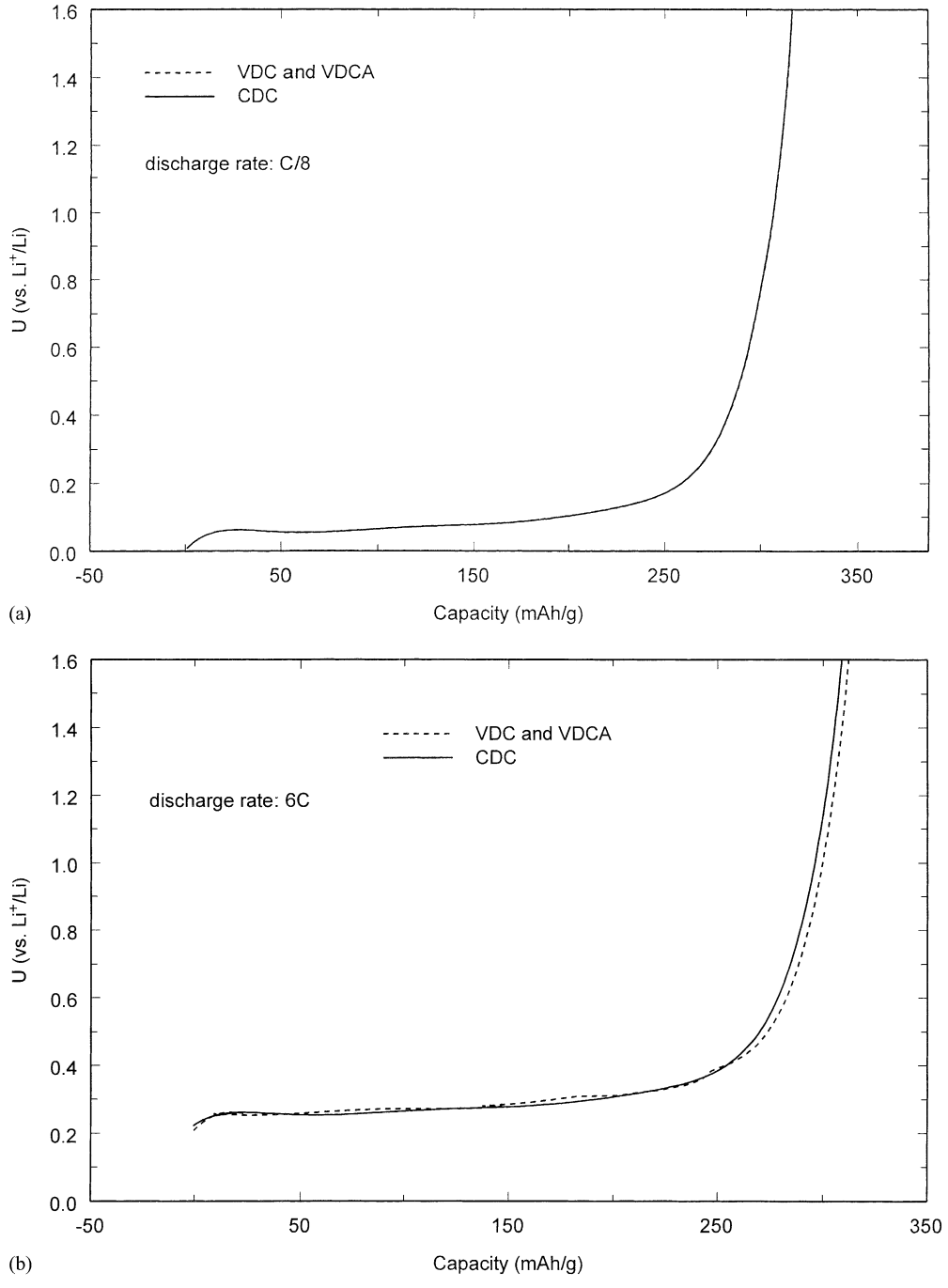

Fig. 4. Comparison of the predicted discharge profiles by the CDC model and the VDC model at different discharge rates.

Table 3
Summary of the parameters used in the simulation

Parameter	Value	Resource
Particle radius (μm)	5	Timcal America (manufacturer)
Diameter of the graphite electrode, D_e (cm)	1.26	Measured
Thickness of the graphite electrode, L (cm)	9.4×10^{-3}	Measured
Mass of the graphite electrode, m_e (g)	0.0099	Measured
Volume of the graphite electrode, V_e (cm^3)	1.17×10^{-2}	Measured
Porosity of the graphite electrode, (ε)	0.35	Assumed
Surface area per unit volume, A_s (cm^2/cm^3)	3.9×10^3	From Eq. (12)
Specific density of graphite, ρ (g/cm^3)	2.21	Timcal America (manufacturer)
Molecular weight of carbon, M_w (g/mol)	12	Assumed
Initial lithium fractional occupancy, X_I^0	0.877	Measured
Site concentration, C_s (mol/cm^3)	0.027	From Eq. (7)
Symmetric factor, β	0.5	[16]
Diffusion coefficient, D_I^0 (cm^2/s)	10^{-11}	Initial guess
Reference exchange current density, $I_{o,ref}$ (mA/g)	10	Initial guess

and VDCA models give the same profile and predict the same value of diffusion coefficient and exchange current. The experimental data were taken every 12 min from a cell that was about three cycles into its life where the system had essentially been stabilized. $I_{o,ref}$ is obtained to be 155 mA/g using non-linear parameter estimation [24,27] and the value of D_I^0 is found to be 1.25×10^{-9} cm^2/s. Note that, when an initial guess of 10 or 1000 mA/g is assumed for $I_{o,ref}$, it converges to 155 mA/g. When an initial guess of 10^{-11} cm^2/s is assumed, D_I^0 converges to 1.25×10^{-9} cm^2/s. However, when an initial guess of 10^{-8} cm^2/s is assumed D_I^0 converges to 10^{-8} cm^2/s. Similarly, when an initial guess 10^{-7} cm^2/s is assumed, D_I^0 converges to 10^{-7} cm^2/s. This means that at C/8 discharge, there is no diffusion limitation and the diffusion coefficient can only be predicted to be $\geq 1.25 \times 10^{-9}$ cm^2/s.

The simulated discharge curves using the CDC, VDC and VDAC model at the rates of C/8 and 4C are displayed in Fig. 4. Note that, the differences in the predicted discharge curves by the VDC model and by the CDC model are only observed at the discharge rate of 4C and above and that even at 6C rates, the approximate solution given in Eq. (17) (VDCA) matches exactly with the numerical solution of VDC model. Therefore, for galvanostatic charge–discharge process of 5 μm particle, under any rate less than 2C, the simple CDC model can replace the VDC model and for rates

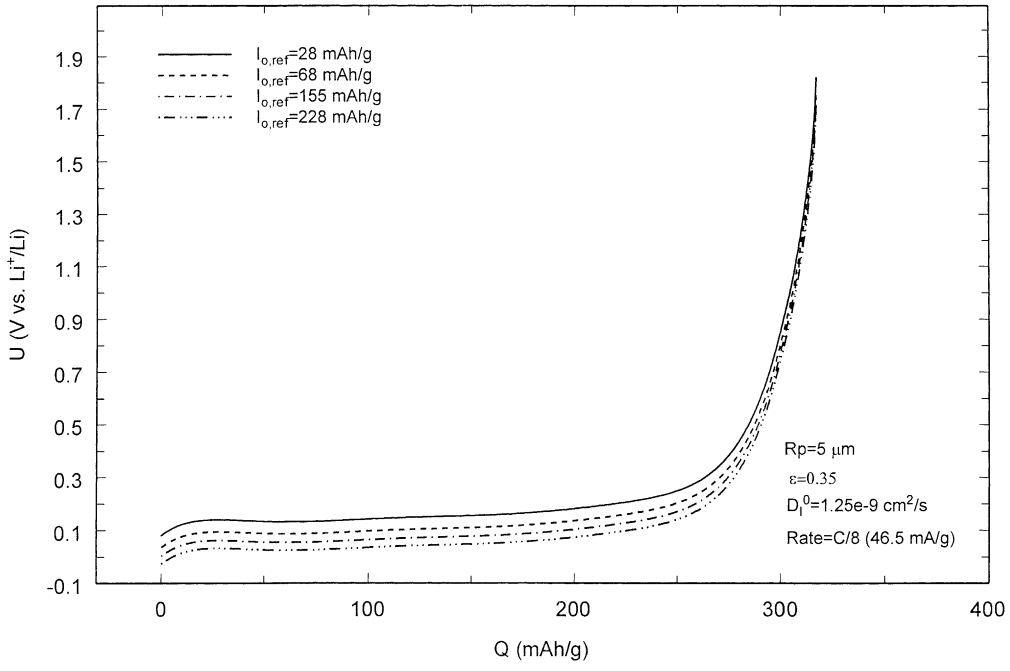

Fig. 5. The effect of exchange current density on the discharge performance of graphite.

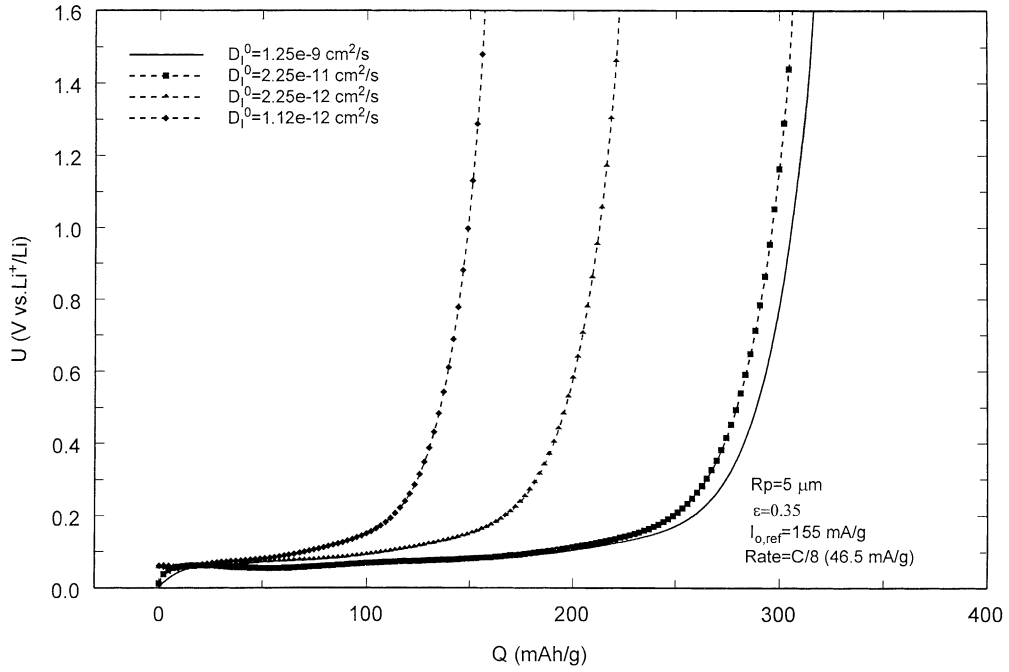

Fig. 6. The effect of diffusion coefficient on the discharge performance of graphite.

up to 6C approximate solution given in Eq. (17) can be used without any loss of accuracy. For particles of radius 10 μm, CDC model is good only till discharge rates of C/2. This is true because, the error involved in the CDC model is based upon Ψ, which increases four times, when the particle size is doubled. And hence, the CDC model is good only for discharge rates less than $2C/4 = C/2$. Similarly, for a particle size of 10 μm, VDCA can be used only for discharge rates less than 1.5C. Note, Ψ is determined to be 0.0024–0.076 for the discharge rate ranging from C/8 to 4C for a 5 μm particle. For higher rates one can obtain approximate and accurate solutions using higher order polynomial profile approximations [25,26]. Note that, at higher discharge rates or for higher particle radius CDC model cannot be used and VDC model has to be used as seen for a 4C discharge in Fig. 4b.

Fig. 5 shows the discharge potential profiles predicted for the Ni-composite coated graphite at different reference exchange current densities. We observe that, the lithium deintercalation potential decreases with increasing exchange currents.

The simulated lithium discharge potential profiles (for a constant C/8 discharge rate and cut off potential) with different diffusion coefficients are presented in Fig. 6 using VDC model. When the diffusion coefficient decreases from 1.25×10^{-9} to 2.25×10^{-11} cm^2/s, the discharge capacity decreases from 316 to 306 mA h/g. The decrease of the diffusion coefficient from 2.25×10^{-11} to 2.25×10^{-12} cm^2/s leads to a large decrease of the capacity from 306 to 222 mA h/g. The experimental operating condition (Fig. 3) is not diffusion limited. One can only conclude that the diffusion coefficient is greater than 1.25×10^{-9} cm^2/s.

5. Conclusions

A simple theoretical model is presented to simulate the galvanostatic discharge behavior of the Ni-composite graphite electrode. The discharge profiles predicted by using a constant diffusion coefficient and by a varied diffusion coefficient are compared in this paper. The results show that, the VDC model can be simplified to the CDC model for rates less than 2C for the given 5 μm particle. Furthermore, for rates up to 6C, an approximate analytical solution is provided for the VDC model. For discharge rates less than 2C, the process is not diffusion limited and hence diffusion coefficient is predicted to be $\geq 1.25 \times 10^{-9}$ cm^2/s and the exchange current is predicted to be 155 mA/g.

References

[1] M.W. Verbrugge, B.J. Koch, J. Electrochem. Soc. 146 (1999) 833.
[2] T.D. Tran, J.H. Feikert, T.W. Pekala, K. Kinoshita, J. Appl. Electrochem. 26 (1996) 1161.
[3] M. Winter, P. Novak, A. Monnier, J. Electrochem. Soc. 145 (1998) 428.
[4] W. Xing, J.R. Dahn, J. Electrochem. Soc. 144 (1997) 1195.
[5] P. Arora, R.E. White, M. Doyle, J. Electrochem. Soc. 145 (1998) 3647.
[6] K. West, T. Jacobsen, S. Atlung, J. Electrochem. Soc. 129 (1982) 1480.
[7] Z. Mao, R.E. White, J. Power Sources 43-44 (1993) 181.
[8] M. Doyle, T.F. Fuller, J. Newman, J. Electrochem. Soc. 140 (1993) 1526.
[9] T.F. Fuller, M. Doyle, J. Newman, J. Electrochem. Soc. 141 (1994) 982.
[10] T.F. Fuller, M. Doyle, J. Newman, J. Electrochem. Soc. 141 (1994) 1.

[11] M. Doyle, T.F. Fuller, J. Newman, A.S. Gozdz, C.N. Schmutz, J. Tarascon, J. Electrochem. Soc. 143 (1996) 1890.
[12] D. Guyomard, J.M. Tarascon, J. Electrochem. Soc. 139 (1992) 937.
[13] N. Takami, A. Satoh, M. Hara, T. Ohsaki, J. Electrochem. Soc. 142 (1995) 371.
[14] T. Uchida, Y. Morikawa, H. Ikuta, M. Wakihara, J. Electrochem. Soc. 143 (1996) 2606.
[15] P. Yu, B.N. Popov, J.A. Ritter, R.E. White, J. Electrochem. Soc., submitted for publication.
[16] M.W. Verbrugge, B.J. Koch, J. Electrochem. Soc. 143 (1996) 600.
[17] M.W. Verbrugge, B.J. Koch, J. Electrochem. Soc. 146 (1999) 833.
[18] P. Yu, J.A. Ritter, R.E. White, B.N. Popov, J. Electrochem. Soc. 147 (2000) 1280.
[19] P. Yu, J.A. Ritter, R.E. White, B.N. Popov, J. Electrochem. Soc. 147 (2000) 2081.
[20] V.R. Subramanian, R.E. White, Tutorials in electrochemical engineering and mathematical modeling, J. Electrochem. Soc. Proc. 99–14 (1999).
[21] H.S. Carslaw, J.C. Jaeger, Conduction of Heat in Solids, Oxford University Press, London, 1973.
[22] V.R. Subramanian, R.E. White, New separation of variables method for composite electrodes with galvanostatic boundary conditions, J. Power Sources 96 (2001) 109–119.
[23] M. Doyle, J. Newman, J. Appl. Electrochem. 27 (1997) 846.
[24] V.R. Subramanian, R.E. White, Solving differential equations with maple, Chem. Eng. Edu., in press.
[25] V.R. Subramanian, J.A. Ritter, R.E. White, Approximate solutions for galvanostatic discharge of electrode particles. 1. Constant diffusion coefficient, submitted for publication.
[26] V.R. Subramanian, J.A. Ritter, R.E. White, Approximate solutions for galvanostatic discharge of electrode particles. 2. Variable diffusion coefficient, J. Electrochem. Soc., in preparation.
[27] A. Constantinides, N. Mostoufi, Numerical Methods for Chemical Engineers with MATLAB Applications, Prentice-Hall PTR, Upper Saddle River, NJ, 1999, p. 491.